Available online at www.sciencedirect.com
ScienceDirect
Journal of Computational and Applied Mathematics 203 (2007) 516–532
JOURNAL OF COMPUTATIONAL AND APPLIED MATHEMATICS
www.elsevier.com/locate/cam

Wick-stochastic finite element solution of reaction–diffusion problems

Hassan Manouzi[a], Mohammed Seaïd[b], Mostafa Zahri[c,*]

[a] *Departement de Mathematiques et Statistique, Universite Laval, Quebec, Canada*
[b] *Fachbereich Mathematik, TU Darmstadt, 64289 Darmstadt, Germany*
[c] *Fachbereich Mathematik, Johann Wolfgang Goethe-Universität, 60054 Frankfurt am Main, Germany*

Received 29 November 2004; received in revised form 22 July 2005

Abstract

Real life reaction–diffusion problems are characterized by their inherent or externally induced uncertainties in the design parameters. This paper presents a finite element solution of reaction–diffusion equations of Wick type. Using the Wick-product properties and the Wiener–Itô chaos expansion, the stochastic variational problem is reformulated to a set of deterministic variational problems. To obtain the chaos coefficients in the corresponding deterministic reaction–diffusion, we implement the usual Galerkin finite element method using standard techniques. Once this representation is computed, the statistics of the numerical solution can be easily evaluated. Computational results are shown for one- and two-dimensional test examples.

MSC: 60H40; 35K57; 78M10; 65M60; 60H35

Keywords: Wick-stochastic partial differential equations; Reaction–diffusion problems; Finite element method; Stochastic simulation; White noise

1. Introduction

Many reaction–diffusion problems in biology and chemistry are modeled by partial differential equations (PDEs). These problems have been extensively studied in the literature and their numerical solution can be accurately computed provided the diffusion coefficients, reaction excitations, initial and boundary data are given in a deterministic way. However, modeling real-life reaction–diffusion systems is complicated by the high heterogeneity of the diffusion process combined with insufficient information characterizing the kinetic reactions. An example concerns the spatio-temporal pattern formation in cell metabolism where the intact living cell is based on a highly complex spatial organization of its constituents. The reactants mediating, and processed by the chemical pathways of cell are heterogeneously distributed through the cytoplasm and cell membranes. The diffusion of reactant species among localized reaction regions within the cell is therefore a central feature of biochemistry. For more details, we refer to [11,5,12] and further references are cited therein.

The uncertainties mentioned above can be conveniently described by random fields, whose statistics are usually inferred from experiments. This requires to include, in the PDEs modeling the problem under consideration, a rational

* Corresponding author.
E-mail address: zahri@math.uni-frankfurt.de (M. Zahri).

0377-0427/$ - see front matter © 2006 Elsevier B.V. All rights reserved.
doi:10.1016/j.cam.2006.04.049

assessment of uncertainty. Consequently, this leads to the notion of stochastic partial differential equations (SPDEs). See the text book [7] for the basics of SPDEs and other related issues. The numerical methods presented in our work can be applied to arbitrary unsteady semilinear SPDEs, and are formulated here for a class of stochastic reaction–diffusion models.

For regular deterministic reaction–diffusion equations, multiplications of the solutions to diffusion and in reaction terms are performed point-valued in ordinary manner. In the stochastic case, this may cause problems and it is hard to give a mathematical meaning of this product since the processes are not smooth. To overcome this drawback, multiplications in the stochastic reaction–diffusion equations are performed using the Wick product. This product can be interpreted as a regularization procedure in order to handle the equations using the Wick calculus [7,9,1,6], and it also provides an extension of Itô integration to more than one dimension. A theory of SPDEs where products between random fields are interpreted as Wick products was developed in [7]. This allows the use of highly irregula r random fields as coefficients in SPDEs and obtain the solution as a stochastic distribution.

The numerical methods used to approximate solutions to stochastic reaction–diffusion equations should be concerned with quantifying uncertainties in diffusion and reaction terms among others. Although Monte Carlo simulations are the most popular techniques to solve such situations, these methods suffer from substantial limitations mainly related to high amount of computational cost and memory storage. In this paper, we propose an alternative approach that combines a finite element method with Wiener–Itô chaos expansions. Using an orthogonal basis generated by direct products of Hermite polynomials with Gaussian random variables, we first decompose an arbitrary stochastic function into a deterministic part and randomness. Then, the stochastic variational problem is transformed to a sequence of deterministic variational problems to be solved for chaos coefficients in the Wiener–Itô expansion. A backward time integration is used in the Galerkin finite element discretization of the problem. Once the chaos coefficients are computed from the deterministic reaction–diffusion equations, the statistical properties of the stochastic solution can be straightforwardly investigated.

Our objective in this work is to implement a robust algorithm for solving SPDEs. The key idea consists on combining the Wiener–Itô chaos expansions with a Galerkin finite element discretization to construct a numerical method for stochastic reaction–diffusion equations. Our method is an extension of the work in Ref. [10] done for steady Wick-stochastic pressure equation. We should mention that the present method has been analyzed in [13] and a priori error estimates of the numerical solution has also been given therein. However, to our knowledge, this is the first time that the method is implemented and experimented for a class of two-dimensional boundary value problems. Numerical illustrations are shown for several examples on both one and two space dimensions. The outline of the paper is as follows. In Section 2, we recall some preliminaries and notations needed for the formulation of our method. Variational formulations and discretizations in time and space are presented in Section 3. Section 4 is devoted to details on the algorithmic implementation of the method. Numerical results and examples are given in Section 5. In Section 6 some concluding remarks are listed.

2. Reaction–diffusion equations of Wick type

Given a probability sample Ω of random events, an open bounded domain $\mathscr{D} \subset \mathbb{R}^d$ ($d = 1, 2$ or 3) with a smooth boundary $\partial\mathscr{D}$ and a time interval $[0, T]$, we are interested in this paper, to approximate solutions to the stochastic reaction–diffusion equations

$$\begin{aligned} &\partial_t u - \operatorname{div}(D(\mathbf{x}, \omega) \diamond \nabla u) = f(t, \mathbf{x}, \omega), \quad (t, \mathbf{x}, \omega) \in (0, T) \times \mathscr{D} \times \Omega, \\ &u(t, \mathbf{x}, \omega) = 0, \quad (t, \mathbf{x}, \omega) \in [0, T] \times \partial\mathscr{D} \times \Omega, \\ &u(0, \mathbf{x}, \omega) = u^0(\mathbf{x}, \omega), \quad (\mathbf{x}, \omega) \in \mathscr{D} \times \Omega, \end{aligned} \tag{1}$$

where $u(t, \mathbf{x}, \omega)$ is, for example, the stochastic concentration of some chemical species, $D(\mathbf{x}, \omega)$ is the stochastic diffusion coefficient which can be a smooth or a very rough positive white noise, $f(t, \mathbf{x}, \omega)$ is the stochastic reaction term and $u^0(\mathbf{x}, \omega)$ is a given initial data. In (1), the symbol $\diamond$ denotes the Wick product which gives a mathematical interpretation of the product of generalized functions. This allows product of two stochastic processes and it is analogous to the problem of multiplying two Schwartz distributions. The Wick product becomes the ordinary product whenever one of the variables in the product is deterministic. Note that the stochastic functions $D(\mathbf{x}, \omega)$ and $f(t, \mathbf{x}, \omega)$ can be independent white Gaussian noises with bounded and continuous expectations. We shall approximate numerical solution to the problem (1) subject to the following assumption:

(A): The diffusion coefficient $D(\mathbf{x}, \omega)$ is uniformly positive definite and essentially bounded in a distribution sense.

We recast our model problem (1) in a weak form. To do so, we consider the usual deterministic Sobolev spaces $H^s(\mathscr{D})$ and $H_0^s(\mathscr{D})$. The dual spaces of $H_0^s(\mathscr{D})$ is denoted by $H^{-s}(\mathscr{D})$. For $s=0$, $H^s(\mathscr{D})$ is the Hilbert space $L^2(\mathscr{D})$ whose inner product and norm are denoted by $(\cdot,\cdot)$ and $\|\cdot\|$, respectively. The dual space of $L^2(\mathscr{D})$ is itself. The probability space Ω of the random variable ω can be defined as follows:

Let $\mathscr{S}(\mathbb{R}^d)$ be the Schwartz space of rapidly decaying $C^\infty(\mathbb{R}^d)$ functions, and $\mathscr{S}'(\mathbb{R}^d)$ be its dual space of tempered distributions. Then, as shown in [7], there is a probability measure μ on the Borel sets $\mathscr{B}(\mathscr{S}'(\mathbb{R}^d))$ such that $\Omega := (\mathscr{S}'(\mathbb{R}^d), \mathscr{B}(\mathscr{S}'(\mathbb{R}^d)), \mu)$ is a probability (white noise) space, and μ the normalized Gaussian measure satisfying

$$\mathbb{E}[\mathrm{e}^{i\langle\cdot,\phi\rangle}] := \int_{\mathscr{S}'(\mathbb{R}^d)} \mathrm{e}^{i\langle\omega,\phi\rangle}\,\mathrm{d}\mu(\omega) = \mathrm{e}^{-(1/2)\|\phi\|^2} \quad \forall\phi\in\mathscr{S}(\mathbb{R}^d),$$

where $\mathbb{E}[\cdot]$ is the expectation operator. The space of random variables with finite variance is denoted by $L^2(\Omega)$.

To construct the Wiener chaos expansion we denote by $\mathscr{I}$ the set of all multi-indices $(\alpha_1,\alpha_2,\ldots)\in\mathbb{N}_0^{\mathbb{N}}$ with only finitely many $\alpha_i\neq 0$, and let $l(\alpha) := \max\{i : \alpha_i\neq 0\}$, $\alpha+\beta := (\alpha_1+\beta_1,\alpha_2+\beta_2,\ldots)$, $\alpha! := \alpha_1!\alpha_2!\ldots$, $|\alpha| := \sum_i \alpha_i$, and $\alpha<\beta$ if $\alpha_i<\beta_i$ for all $i\in\mathbb{N}$. For $n\in\mathbb{N}_0$, $x\in\mathbb{R}$ define the Hermite polynomial

$$h_n(x) = (-1)^n \mathrm{e}^{x^2/2}\frac{\mathrm{d}^n}{\mathrm{d}x^n}(\mathrm{e}^{-x^2/2}),$$

and for $n\in\mathbb{N}$ we define the Hermite functions

$$\xi_n = \pi^{-1/4}((n-1)!)^{-1/2}\mathrm{e}^{-x^2/2}h_{n-1}(\sqrt{2}x).$$

Define the tensor-product

$$\xi_\delta(\mathbf{x}) := \xi_{\delta_1}\otimes\xi_{\delta_2}\otimes\cdots\otimes\xi_{\delta_d}(\mathbf{x}) = \xi_{\delta_1}(x_1)\otimes\xi_{\delta_2}(x_2)\otimes\cdots\otimes\xi_{\delta_d}(x_d).$$

For $\alpha\in\mathscr{I}$, define the stochastic variable

$$H_\alpha(\omega) = \prod_{j=1}^{l(\alpha)} h_{\alpha_j}(\langle\omega,\xi_{\delta_j}\rangle), \quad \omega\in\mathscr{S}'(\mathbb{R}^d),$$

where δ_j is some ordering of d-dimensional multi-indices such that $i<j \Longrightarrow |\delta_i|<|\delta_j|$. From [7], the family $\{H_\alpha\}_{\alpha\in\mathscr{I}}$ constitutes an orthogonal basis for $L^2(\Omega)$, with $\mathbb{E}[H_\alpha H_\beta] = \delta_{\alpha\beta}\alpha!$. Thus, any function $f\in L^2(\Omega)$ has a unique representation (Wiener–Itô chaos expansion)

$$f = \sum_{\alpha\in\mathscr{I}} f_\alpha H_\alpha, \quad \|f\|^2_{L^2(\Omega)} := \int_\Omega f(\omega)^2\,\mathrm{d}\mu(\omega) = \sum_{\alpha\in\mathscr{I}} f_\alpha^2\alpha!.$$

Here $f_\alpha\in\mathbb{R}$ denotes the αth chaos coefficient of function f. Let V denotes any real separable Hilbert space with inner product $(\cdot,\cdot)_V$ and let $k\in\mathbb{R}$ and $\rho\in[0,1]$. Define

$$(\mathscr{S})^{\rho,k,V} := \left\{ f=\sum_{\alpha\in\mathscr{I}} f_\alpha H_\alpha :\ f_\alpha\in V\ \forall\alpha\in\mathscr{I} \text{ and } \|f\|_{\rho,k,V}<\infty \right\},$$

where the norm $\|\cdot\|_{\rho,k,V}$ is induced by the inner product

$$(f,g)_{\rho,k,V} := \sum_{\alpha\in\mathscr{I}} (f_\alpha,g_\alpha)(\alpha!)^{1+\rho}(2\mathbb{N})^{k\alpha}, \quad f,g\in(\mathscr{S})^{\rho,k,V}, \tag{2}$$

where $(2\mathbb{N})^{k\alpha} = \prod_j (2j)^{k\alpha_j}$. Here $(\mathscr{S})^{\rho,k,V}$ is called the Kondratiev space of test functions and its dual is denoted $(\mathscr{S})^{-\rho,-k,V'}$, and is the Kondratiev space of distributions [9,2]. The dual parity between $(\mathscr{S})^{-\rho,-k,V'}$ and $(\mathscr{S})^{\rho,k,V}$ is defined by

$$\langle F,f\rangle := \int_\Omega F(\omega)f(\omega)\,\mathrm{d}\mu(\omega) = \sum_{\alpha\in\mathscr{I}} F_\alpha f_\alpha\alpha!.$$

For simplicity in the presentation we use the notations $(\mathscr{S})^{\rho,k,s,\mathscr{D}}$ and $(\mathscr{S})_0^{\rho,k,s,\mathscr{D}}$ to denote $(\mathscr{S})^{\rho,k,H^s(\mathscr{D})}$ and $(\mathscr{S})^{\rho,k,H_0^s(\mathscr{D})}$, respectively, and we omit the parameters ρ, k, s and the domain $\mathscr{D}$ whenever it is clear from the context. From [13], we have for $\rho \in [-1, 1]$

$$(\mathscr{S})_0^{\rho,k,1} \hookrightarrow (\mathscr{S})^{\rho,k,0} \hookrightarrow (\mathscr{S})^{-\rho,-k,-1}.$$

Let $f = \sum_{\alpha\in\mathscr{I}} f_\alpha H_\alpha \in (\mathscr{S})^{\rho,k,s,\mathscr{D}}$ and $\beta \in \mathbb{N}_0^d$ with $|\beta| \leqslant s$. Then the derivative $D^\beta f$ is defined as

$$D^\beta f := \sum_{\alpha\in\mathscr{I}} D^\beta f_\alpha H_\alpha, \tag{3}$$

where $D^\beta f_\alpha$ is the derivative in the usual weak sense. Hence from the definition of the inner product (2) and (3)

$$(f, g)_{\rho,k,1} = (f, g)_{\rho,k,0} + (\nabla f, \nabla g)_{\rho,k,0} \quad \forall f, g \in (\mathscr{S})^{\rho,k,1}.$$

Here $(\cdot,\cdot)_{\rho,k,1}$ and $(\cdot,\cdot)_{\rho,k,0}$ denote the inner products in $(\mathscr{S})^{\rho,k,1}$ and $(\mathscr{S})^{\rho,k,0}$, respectively.

Next we recall the definition of Wick product [7]. Given $f = \sum_{\alpha\in\mathscr{I}} f_\alpha H_\alpha$ and $g = \sum_{\beta\in\mathscr{I}} g_\beta H_\beta$ two formal serieses, the Wick product $f \diamond g$ is defined as

$$f \diamond g := \sum_{\alpha,\beta\in\mathscr{I}} f_\alpha g_\beta H_{\alpha+\beta}.$$

The Wick product satisfies the commutative, associative and distributive laws. Thus, both $(\mathscr{S})^{\rho,k,V}$ and $(\mathscr{S})^{-\rho,-k,V'}$ are algebras with the Wick product as multiplication, compare [15]. Furthermore, for any formal sum $f = \sum_{\alpha\in\mathscr{I}} f_\alpha H_\alpha$, the zeroth order chaos coefficient $f_0 := \mathbb{E}[f]$ and referred to as the generalized expectation. Note that $\mathbb{E}[f \diamond g] = \mathbb{E}[f]\mathbb{E}[g]$ for any given pair of (generalized) stochastic variables f and g. This property does not hold for the ordinary product.

3. Wick-stochastic finite element method

3.1. Variational formulation

The starting point of finite element method is the variational formulation of Eqs. (1) which requires spaces that incorporate time dependency. To this end, given a pair of Hilbert spaces X and Y such that $Y \hookrightarrow X \hookrightarrow Y'$, we define

$$W(0, T; Y) := \{f \in L^2(0, T; Y) : \partial_t f \in L^2(0, T; Y)\}.$$

It has been shown in [3] that $W(0, T; Y)$ forms a Hilbert space with respect to the inner product

$$(f, g)_{W(0,T;Y)} := \int_0^T (f(s), g(s))_Y \, ds + \int_0^T (\partial_t u(s), \partial_t v(s))_{Y'} \, ds,$$

and $W(0, T; Y) \hookrightarrow C^0(0, T; X)$, where $C^0(0, T; X)$ is the space of continuous functions from $[0, T]$ into X. We also introduce the bilinear form

$$\mathscr{A}(u, v) := (D \diamond \nabla u, \nabla v) \quad \forall u, v \in V.$$

We define the variational (weak) formulation of Eqs. (1) as follows:

Find $u \in W(0, T; V)$ such that

$$(\partial_t u, v) + \mathscr{A}(u, v) = (f, v) \quad \forall v \in V$$

$$u(0) = u^0. \tag{4}$$

The following results have been proven in [13,16].

Lemma 1. *Suppose that the diffusion coefficient D satisfies the assumption* (A). *Then the bilinear form $\mathscr{A}$ satisfies the following properties*:

(i) *The function $t \longmapsto \mathscr{A}(u, v)$ is measurable $\forall u, v \in V$.*

(ii) *There exists a constant C such that*

$$|\mathscr{A}(u,v)| \leqslant C\|u\|\|v\| \quad \forall t \in [0,T] \text{ and } u, v \in V. \tag{5}$$

(iii) *If the coefficient D is small enough, there exist positive constants* α *and* γ *such that*

$$\mathscr{A}(v,v) \geqslant \alpha\|v\|^2 - \gamma\|v\|^2 \quad \forall t \in [0,T] \text{ and } v \in V.$$

In what follows we establish the relation between the weak formulation (4) and the corresponding system of deterministic variational problems for the chaos coefficients u_γ with $\gamma \in \mathscr{I}$. Let

$$D = \sum_{\gamma\in\mathscr{I}} D_\gamma H_\gamma, \quad u^0 = \sum_{\gamma\in\mathscr{I}} u_\gamma^0 H_\gamma,$$

and define the bilinear form $\mathscr{B}_\beta(f,g)$ as

$$\mathscr{B}_\beta(f,g) = (D_\beta \nabla f, \nabla g)_0 \quad \forall f, g \in H_0^1(\mathscr{D}).$$

It has been shown in [1] that there exists a constant $0 < M_\beta < \infty$, independent of t such that

$$|\mathscr{B}_\beta(f,g)| \leqslant M_\beta \|f\|_1 \|g\|_1 \quad \forall t \in [0,T] \text{ and } f, g \in H_0^1(\mathscr{D}). \tag{6}$$

Theorem 1. *Let* $u = \sum_{\gamma\in\mathscr{I}} u_\gamma H_\gamma$ *be the solution of the variational problem* (4). *Then the chaos coefficients* u_γ *of u satisfy the following system of variational problems*:

(i) *If* $\gamma = 0$, *find* $u_\gamma \in H_0^1(\mathscr{D})$ *such that*

$$\begin{aligned} &(\partial_t u_\gamma, w) + \mathscr{B}_0(u_\gamma, w) = (f_\gamma, w) \quad \forall w \in H_0^1(\mathscr{D}),\\ &u_\gamma(0) = u_\gamma^0. \end{aligned} \tag{7}$$

(ii) *If* $\gamma \succ 0$, *find* $u_\gamma \in H_0^1(\mathscr{D})$ *such that*

$$\begin{aligned} &(\partial_t u_\gamma, w) + \mathscr{B}_0(u_\gamma, w) = (f_\gamma, w) - \sum_{\alpha<\gamma} \mathscr{B}_{\gamma-\alpha}(u_\alpha, w) \quad \forall w \in H_0^1(\mathscr{D}),\\ &u_\gamma(0) = u_\gamma^0. \end{aligned} \tag{8}$$

Proof. Assume that u solves (4). Then, in particular

$$\begin{aligned} &(\partial_t u, v) + (D \diamond \nabla u, \nabla v) = (f, v),\\ &u(0) = u^0, \end{aligned}$$

holds for $v = wH_\gamma(2\mathbb{N})^{-k\gamma}$ with $w \in H_0^1(\mathscr{D})$, $\gamma \in \mathscr{I}$ and $t \in [0,T]$, i.e.,

$$(\partial_t u_\gamma, w) + ((D \diamond \nabla u)_\gamma, \nabla w) = (f_\gamma, w).$$

By definition of the Wick product we get

$$(\partial_t u_\gamma, w) + \sum_{\alpha+\beta=\gamma} (D_\beta \nabla u_\alpha, \nabla w) = (f_\gamma, w),$$

which is equivalent to

$$(\partial_t u_\gamma, w) + \sum_{\alpha\preceq\gamma} (D_{\gamma-\alpha} \nabla u_\alpha, \nabla w) = (f_\gamma, w).$$

Hence, if $\gamma = 0$ we have also $\alpha = 0$ and we get (7). On the other hand if $\gamma \succ 0$, we may write

$$\sum_{\alpha \preceq \gamma} (D_{\gamma-\alpha} \nabla u_\alpha, \nabla w) = (D_0 \nabla u_\gamma, \nabla w) + \sum_{\alpha \prec \gamma} (D_{\gamma-\alpha} \nabla u_\alpha, \nabla w),$$

from which we deduce (8). □

As a consequence of Theorem 1, we may order the set of multi-indices in such a way that when we reach the γth variational problem in (8), we have already solved the variational problems corresponding to all multi-indices α such that $\alpha \prec \gamma$.

For $N, K \in \mathbb{N}$ we define the cutting $\mathscr{I}_{N,K} \subset \mathscr{I}$ as

$$\mathscr{I}_{N,K} = \{0\} \cup \bigcup_{n=1}^{N} \bigcup_{k=1}^{K} \{\alpha \in \mathbb{N}_0^k : |\alpha| = n \text{ and } \alpha_k \neq 0\}. \tag{9}$$

The resulting space is given by

$$(\mathscr{S}_{N,K})_0^{-1,k,1} := \left\{ f = \sum_{\alpha \in \mathscr{I}_{N,K}} f_\alpha H_\alpha : f_\alpha \in H_0^1(\mathscr{D}),\ \|f\|_{-1,k,1} < \infty \right\}.$$

It is clear that the set $\mathscr{I}_{N,K}$ contains $(N+K)!/N!K!$ multi-indices and $(\mathscr{S}_{N,K})_0^{-1,k,1}$ is a subspace of V for any choice of N and K.

3.2. Fully discrete problem

For the discretization of the space domain $\bar{\mathscr{D}} := \mathscr{D} \cup \partial\mathscr{D}$ we proceed as follows: given h_0, $0 < h_0 < 1$, let h be a space discretization parameter such that $0 < h < h_0$. We generate a quasi-uniform partition $\mathscr{D}_h \subset \bar{\mathscr{D}}$ of small elements $\mathscr{K}_j$ that satisfies the following conditions:

(i) $\bar{\mathscr{D}} = \bigcup_{j=1}^{Ne} \mathscr{K}_j$, where Ne is the number of elements of $\mathscr{D}_h$.
(ii) If $\mathscr{K}_j$ and $\mathscr{K}_l$ are two different elements of $\mathscr{D}_h$, then

$$\mathscr{K}_j \cap \mathscr{K}_l = \begin{cases} P_{jl} & \text{a mesh point, or} \\ \Gamma_{jl} & \text{a common side, or} \\ \emptyset & \text{empty set.} \end{cases}$$

The conforming family of finite element subspaces for the approximate solution is

$$V_h = \{u_h \in C^0(\bar{\mathscr{D}}) : u_h|_{\mathscr{K}_j} \in \mathscr{R}(\mathscr{K}_j)\ \forall j = 1, \ldots, Ne\},$$

where $\mathscr{R}(\mathscr{K}_j)$ are spaces of polynomials defined on $\mathscr{K}_j$. In the literature of finite elements, $\mathscr{R}(\mathscr{K}_j)$ is $P_2(\mathscr{K}_j)$ if the elements of $\mathscr{D}_h$ are simplexes, whereas $\mathscr{R}(\mathscr{K}_j)$ is $Q_2(\mathscr{K}_j)$ if the elements of $\mathscr{D}_h$ are quadrilaterals.

A semi-discrete approximation of (4) is formulated as:

Find $u_h \in W(0, T; V_h)$ such that

$$\begin{aligned} &(\partial_t u_h, v_h) + \mathscr{A}(u_h, v_h) = (f, v_h) \quad \forall v_h \in V_h, \\ &u_h(0) = P_h u_0, \end{aligned} \tag{10}$$

where P_h denotes the H orthogonal projection onto V_h. To discretize the semi-discrete equations (4) in time we use backward Euler scheme because of its simplicity and unconditional stability. However, other time integration schemes can be implemented in a similar manner.

Hence, we divide the time interval $[0, T]$ into subintervals $[t_n, t_{n+1}]$ of length Δt such that $t_n = n\Delta t$. We use U_h^n to denote the point-value of the function u at $(t_n, \mathbf{x}_h)$. Thus, a fully discrete approximation of (4) is formulated as:

Find $U_h^n \in W(0, T; V_h)$, $n = 0, 1, \ldots,$ such that

$$\left(\frac{U_h^{n+1} - U_h^n}{\Delta t}, v_h\right) + \mathscr{A}(U_h^{n+1}, v_h) = (F_h^{n+1}, v_h) \quad \forall v_h \in V_h,$$

$$U_h(0) = P_h u_0. \tag{11}$$

Thus, if U_h^{n+1} solves the problem (11), then the chaos coefficients $\{U_{h,\gamma}^{n+1} : \gamma \in \mathscr{I}_{N,K}\}$ solve the following set of variational problems:

For each $\gamma \in \mathscr{I}_{N,K}$ and $n = 0, 1, \ldots,$ find $U_{h,\gamma}^{n+1} \in V_h$ such that

$$\left(\frac{U_{h,\gamma}^{n+1} - U_{h,\gamma}^n}{\Delta t}, w_h\right) + \mathscr{B}_0(U_{h,\gamma}^{n+1}, w_h) = (F_{h,\gamma}^{n+1}, w_h) - \sum_{\alpha<\gamma} \mathscr{B}_{\gamma-\alpha}(U_{h,\alpha}^{n+1}, w_h) \quad \forall w_h \in V_h,$$

$$U_{h,\gamma}(0) = P_h u_0.$$

Note that a convergence analysis along with a priori error estimates has been established in [13] for the semi-discrete equations (10) and the fully discrete problem (11). Following the same arguments in [13], this analysis can be extended for other implicit time discterization. For instance, the second-order Crank Nicolson method.

4. Solution procedure and implementation

Let M be the number of mesh points of the partition $\mathscr{D}_h$, then any element ψ_h of V_h is expressed as

$$\psi_h = \sum_{j=1}^{M} \psi_j \xi_j(\mathbf{x}),$$

where $\psi_j = \psi_h(\mathbf{x}_j)$, $\mathbf{x}_j$ being the jth mesh point, $\{\xi_j\}$ are the sets of global nodal basis functions of V_h characterized by the property $\xi_j(\mathbf{x}_i) = \delta_{ji}$, with δ_{ji} is the Kronecker delta.

We approximate the finite element solution to U_h^n as

$$U_{h,\gamma}^n = \sum_{j=1}^{M} U_{h,\gamma,j}^n \psi_j. \tag{12}$$

By virtue of definitions of the operators given above, it follows that the fully discrete equations (7)–(8) become:

For each $\gamma \in \mathscr{I}_{N,K}$, solve for $\mathbf{U}_\gamma^{n+1}$

$$(\mathbf{M}_\gamma + \Delta t \mathbf{S}_\gamma)\mathbf{U}_\gamma^{n+1} = \mathbf{M}_\gamma \mathbf{U}_\gamma^n + \Delta t \left(\mathbf{F}_\gamma^{n+1} - \sum_{\alpha<\gamma} \mathbf{S}_{\gamma-\alpha}\mathbf{U}_\alpha^{n+1}\right), \tag{13}$$

where $\mathbf{U}_\gamma^{n+1}$, $\mathbf{U}_\gamma^n$ and $\mathbf{F}_\gamma^{n+1}$ are M-vectors with entries $U_{\gamma,j}^{n+1}$, $U_{\gamma,j}^n$ and $F_{\gamma,j}^{n+1}$, $j = 1, \ldots, M$, respectively. $\mathbf{M}_\gamma$ and $\mathbf{S}_\gamma$ are sparse $M \times M$-matrices the elements of which are given by

$$M_{\gamma,ij} = \int_{\mathscr{D}} \psi_{\gamma,i}\psi_{\gamma,j}\,\mathrm{d}\mathbf{x} \quad \text{and} \quad S_{\gamma,ij} = \int_{\mathscr{D}} D_\gamma \nabla\psi_{\gamma,i}\nabla\psi_{\gamma,j}\,\mathrm{d}\mathbf{x}, \quad i, j = 1, \ldots, M,$$

respectively. Note that $\mathbf{M}_\gamma$ is known as mass matrix in the finite element literature. It is a positive definite matrix with a low condition number, independent of h, so that it is very easy to invert even by the diagonal preconditioned conjugate gradient. The matrix $\mathbf{S}_\gamma$ is known as stiffness matrix in the finite element literature. It has a condition number of $\mathcal{O}(C/h^2)$, where C is a bounded constant. For small h, this condition requires efficient iterative solvers for the linear system (13).

Once the chaos coefficients $\{U_{h,\gamma} : \gamma \in \mathscr{I}_{N,K}\}$ are calculated, stochastic simulations of the solution can be carried out as follows. First, generate R independent standard Gaussian variables $X(\omega) = (X_i(\omega))_{i=1,\ldots,R}$ using some random number generator, and then form the sums

$$u_h(t_n, \omega) = \sum_{\alpha \in \mathscr{I}_{N,K}} U_{h,\alpha}^n H_\alpha(X(\omega)),$$

where

$$H_\alpha(X(\omega)) = \prod_{j=1}^{R} h_{\alpha_j}(X_j(\omega)).$$

Now we are in a position to complete the implementation of our algorithm. The resulting Wick-stochastic finite element method we consider for numerical solution of the reaction–diffusion problem (1) consists of the following three main steps:

For $n = 0, 1, \ldots,$ do:

Step 1:

(i) Construct the ordered cutting $\mathscr{I}_{N,K}$ as in (9) and set $\gamma = (0, \ldots, 0)$.
(ii) Compute the vectors $\mathbf{U}_0^n$, $\mathbf{U}_0^{n+1}$ and $\mathbf{F}_0^{n+1}$.

Step 2: While $\gamma \in \mathscr{I}_{N,K}$ do:

(i) Locate the subset $\mathscr{I}_\gamma = \{\alpha \in \mathscr{I}_{N,K} : \alpha < \gamma\}$.
(ii) Compute the sum $\mathbf{b}_\gamma = \sum_{\alpha<\gamma} \mathbf{S}_{\gamma-\alpha}\mathbf{U}_\alpha^{n+1}$.
(iii) Update the right-hand side $\mathbf{b}_\gamma = \mathbf{M}_\gamma \mathbf{U}_\gamma^n + \Delta t\,(\mathbf{F}_\gamma^{n+1} - \mathbf{b}_\gamma)$.
(iv) Solve for $\mathbf{U}_\gamma^{n+1}$ the linear system: $(\mathbf{M}_\gamma + \Delta t \mathbf{S}_\gamma)\mathbf{U}_\gamma^{n+1} = \mathbf{b}_\gamma$.
(v) Find the next multi-index γ and go to *Step* 2. Check convergence in time: if $n\Delta t \geqslant T$ go to *Step* 3.

Step 3:

(i) Reconstruct the simulations of the solution as follows:
  (a) Generate a sequence $\{X_i, i = 1, \ldots, R^2\}$ of independent Gaussian variables.
  (b) For each $r = 1, \ldots, R$
  Set $X^{(r)} = [X_{(r-1)K+j}],\ \ j = 1, \ldots, R$

  Form realizations of the solution

$$u^{(r)}(t_{n+1}, \mathbf{x}_h) = \sum_{\alpha \in \mathscr{I}_{N,K}} U_\alpha^{n+1}(\mathbf{x}_h) H_\alpha(X^{(r)}).$$

(ii) Perform some statistics and display the results.

Note that, in the above algorithm, the three steps are independent. *Steps* 1 and 3 can be viewed as preprocessing and postprocessing procedures, respectively. Whereas, *Step* 2 represents the main stage of the algorithm that solves a system of $M((N + K)!/N!K!)$ algebraic equations. The *Step* 2(iv) can be solved using the simple LU factorization as in [10]. However, this solver needs explicit storage of the matrices $\mathbf{M}_\gamma$ and $\mathbf{S}_\gamma$ which may limits the robustness of the algorithm. An efficient technique is to use the Krylov-subspace methods. These solvers do not require the explicit storage of the iterative matrices. All what is needed, however, is a subroutine that performs a matrix–vector multiplication, see [8] for details on implementation of Krylov-subspace methods.

5. Numerical examples

In this section, we perform some numerical tests in Eqs. (1). Although results we present here concern academic examples only, the method extends to more realistic problems without major conceptual modifications. Numerical experiments show that zeroth- and first-order Hermite polynomials do not provide a good approximation but in most cases there is no need to go beyond fourth- or fifth-order Hermite polynomials in the Wiener chaos expansions. Therefore, for all the results presented in this section, we used the cutting set $\mathscr{I}_{1,4}$ with five different multi-indices. The computational domain is divided into uniform mesh of elements with mesh size h. To solve the linear system (13) we used the preconditioned Bicgstab method [14] with diagonal preconditioning and a tolerance of 10^{-5} to stop iterations. The following test examples are selected:

Test 1: $D = \mathrm{e}^{\diamond \dot{W}(\mathbf{x})}$ and $f = 0$.

Test 2: $D = 0.1$ and $f = 1 + \dot{W}(\mathbf{x})$.

Test 3: $D = \mathrm{e}^{\diamond \dot{W}(\mathbf{x})}$ and $f = 1 + \dot{W}(\mathbf{x})$.

Here $\dot{W}(\mathbf{x})$ denotes the white noise (formal derivative of Wiener process). It is numerically approximated using the Fourier modes as proposed in [4].

In all our computations the time stepsize Δt is fixed to 10^{-4} and initial condition is taken as a normal distribution centered in the spatial domain $\mathscr{D}$ and with variance equal to 0.01.

5.1. One-dimensional results

We start by running our code for the one-dimensional cases. The space domain is the interval $\mathscr{D} = [0, 1]$ discretized into *Nx* uniform gridpoints. We carry out 100 realizations for each test, then we display the averaged solutions along with some selected simulations.

In Fig. 1 we plot the results obtained by six different realizations (plotted by solid lines) for *Test* 1 at $t = 0.005$. In this figure, we also show the averaged solution (plotted by dotted lines) for comparison reasons. As can be seen, the computed averaged solution preserves the symmetry in the computational domain and, at every realization, the simulated solution remains close to the averaged one. The evolution in time of averaged solution is shown in the left column of Fig. 2 at times $t = 0$, 0.005 and 0.1. The method resolves the diffusive effects accurately without any nonphysical oscillations.

In order to examine the behavior of the numerical solution with respect to the mesh refining, we plot in the right column of Fig. 2 the averaged solution at $t = 0.005$ using a uniform mesh with different number of gridpoints. The convergence of our method is clearly seen as the number of gridpoints increases. In addition, we have observed that solutions obtained by a mesh with 160 gridpoints overlap those obtained by the mesh with 80 gridpoints. Therefore, a mesh of 100 gridpoints as the one used in our computations, is sufficient to provide accurate and efficient solution for the problem under consideration. Needless to say that refining the grids requires more computational work since large linear systems have to be solved at each time step in the algorithm.

Next, we run our code for the *Test* 2 using the same tools to display the results. Thus, in Fig. 3 we plot six different realizations at $t = 0.001$ and in Fig. 4 we show time evolution of the averaged solution (left column) and its behavior on different mesh refinings (right column). The stochastic fluctuations are more visible for *Test* 2 than *Test* 1, compare the results shown in Fig. 3. This is due to the noise introduced by the reaction term f in the reaction–diffusion equation (1). Note that, even with a large diffusion coefficient as the one we used, it was not possible to damp these fluctuations as usually happened in deterministic reaction–diffusion problems. In addition, the initial data in *Test* 2 diffuses with roughly the same rate as in *Test* 1 but still the symmetry of the averaged solution is preserved in the computational domain, see left column in Fig. 4.

Now we turn to compute solutions of *Test* 3. In this example, both the diffusion coefficient and the reaction term contain stochastic effects. As in the previous tests, Fig. 5 shows six different realizations at time $t = 0.005$, whereas Fig. 6 displays the evolution of the averaged solution at different instants (left column) and gridpoints (right column). The computed results offer similar behavior as in *Test* 2.

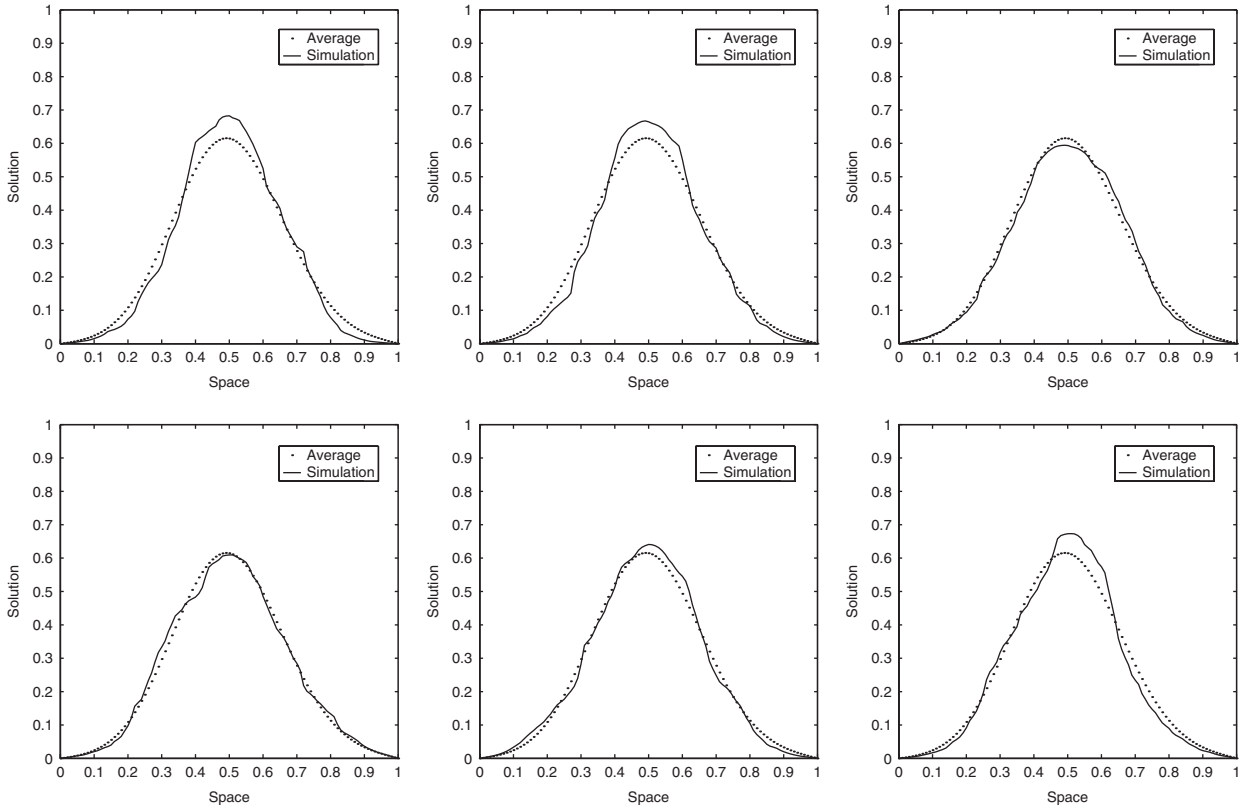

Fig. 1. One-dimensional *Test* 1: six different simulations at time $t = 0.005$.

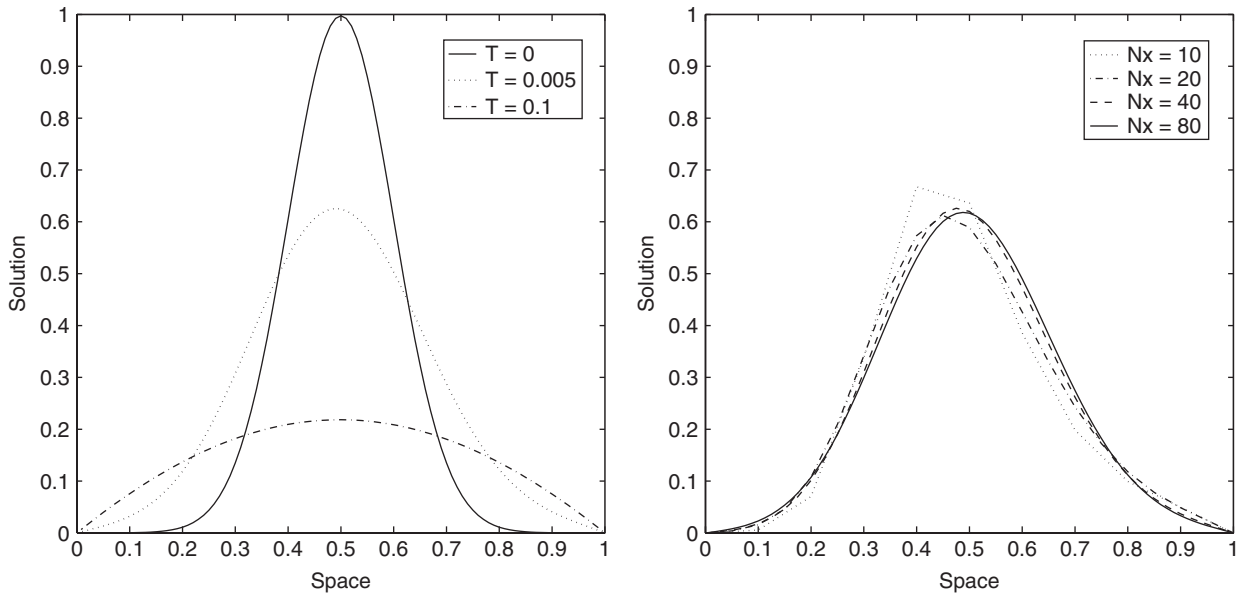

Fig. 2. One-dimensional *Test* 1: averaged solution at different times with $Nx = 100$ (left column) and with different mesh points at time $t = 0.005$ (right column).

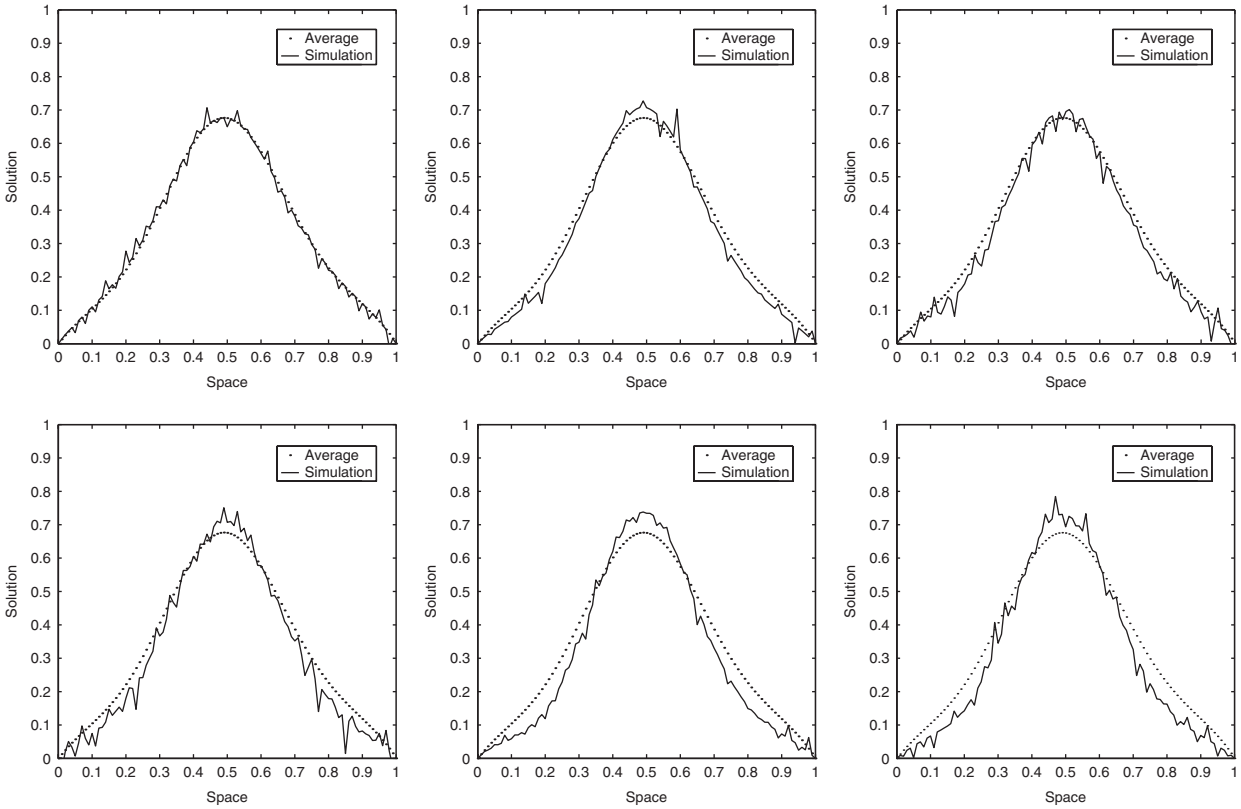

Fig. 3. One-dimensional *Test* 2: six different simulations at time $t = 0.001$.

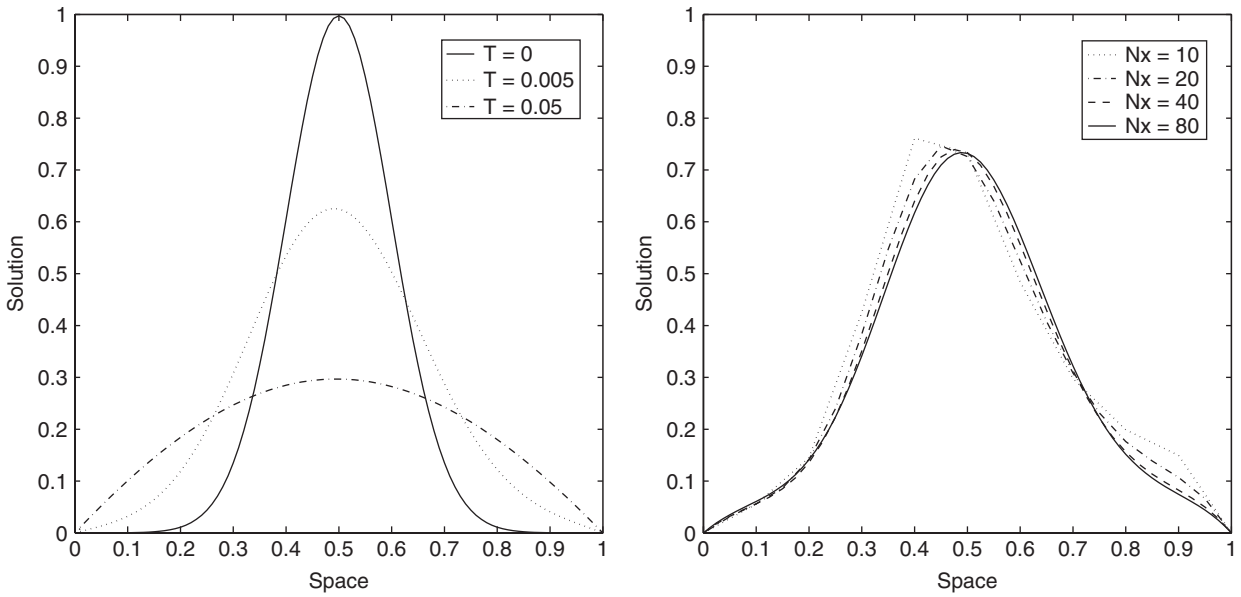

Fig. 4. One-dimensional *Test* 2: averaged solution at different times with $Nx = 100$ (left column) and with different mesh points at time $t = 0.001$ (right column).

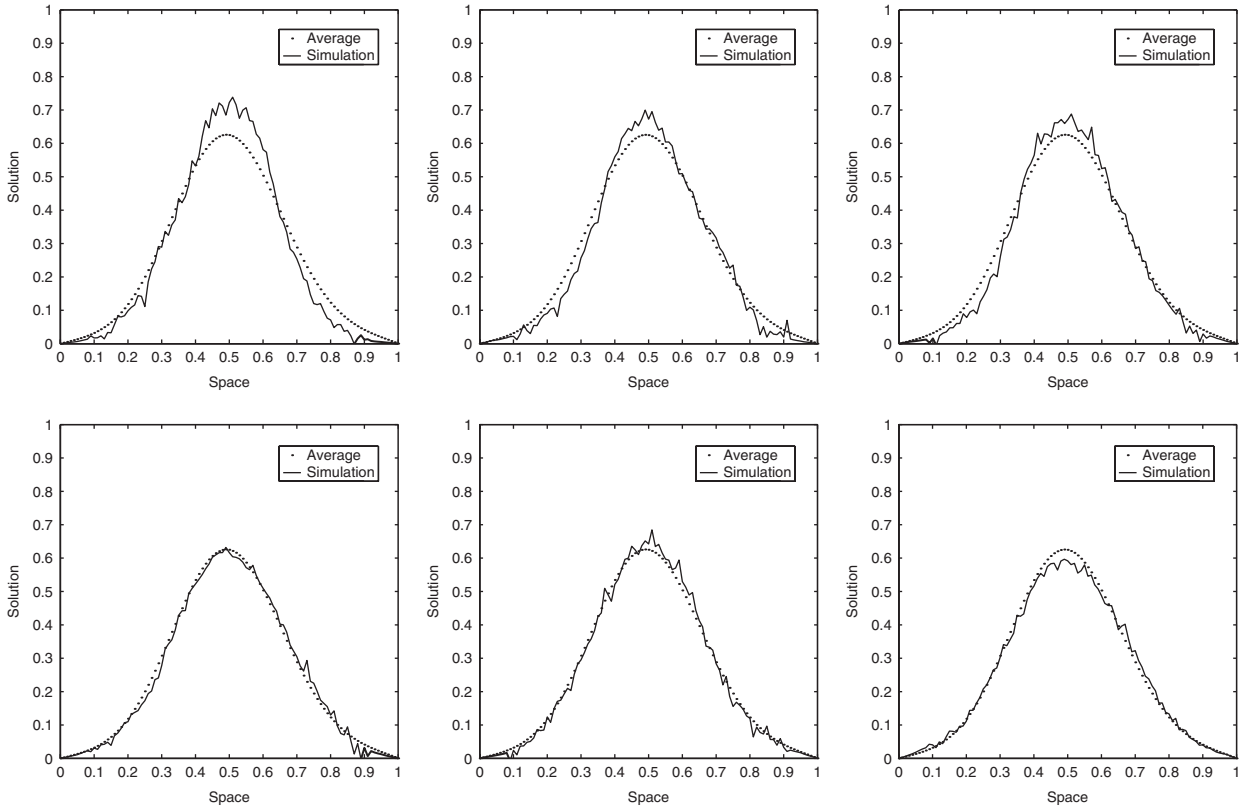

Fig. 5. One-dimensional *Test* 3: six different simulations at time $t = 0.005$.

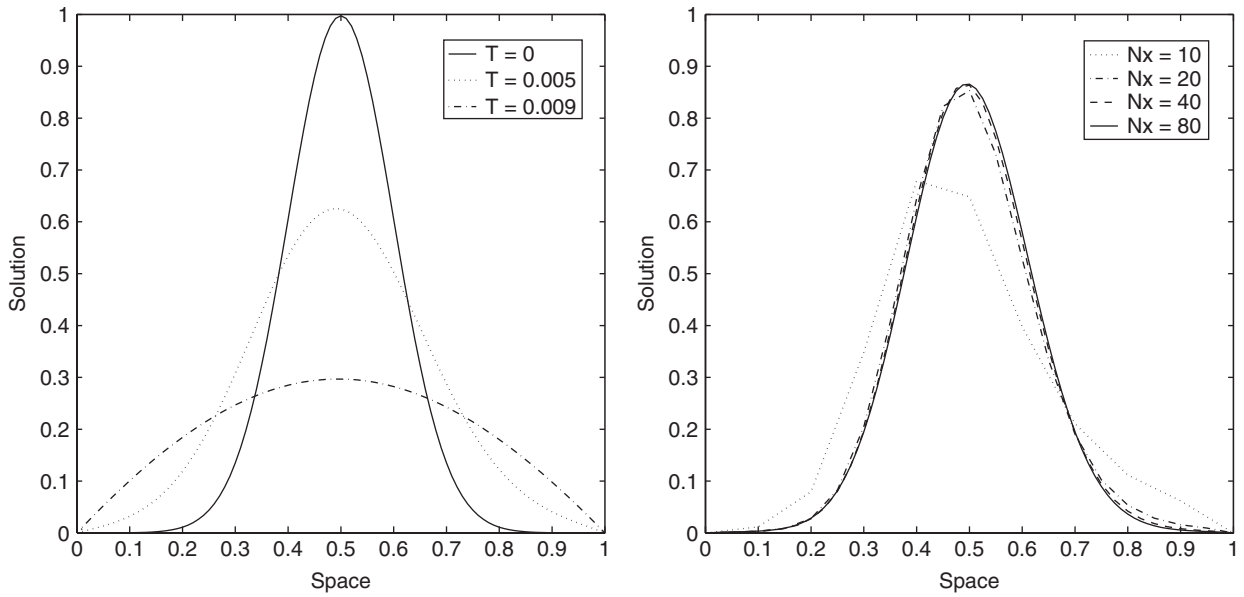

Fig. 6. One-dimensional *Test* 3: averaged solution at different times with $Nx = 100$ (left column) and with different mesh points at time $t = 0.001$ (right column).

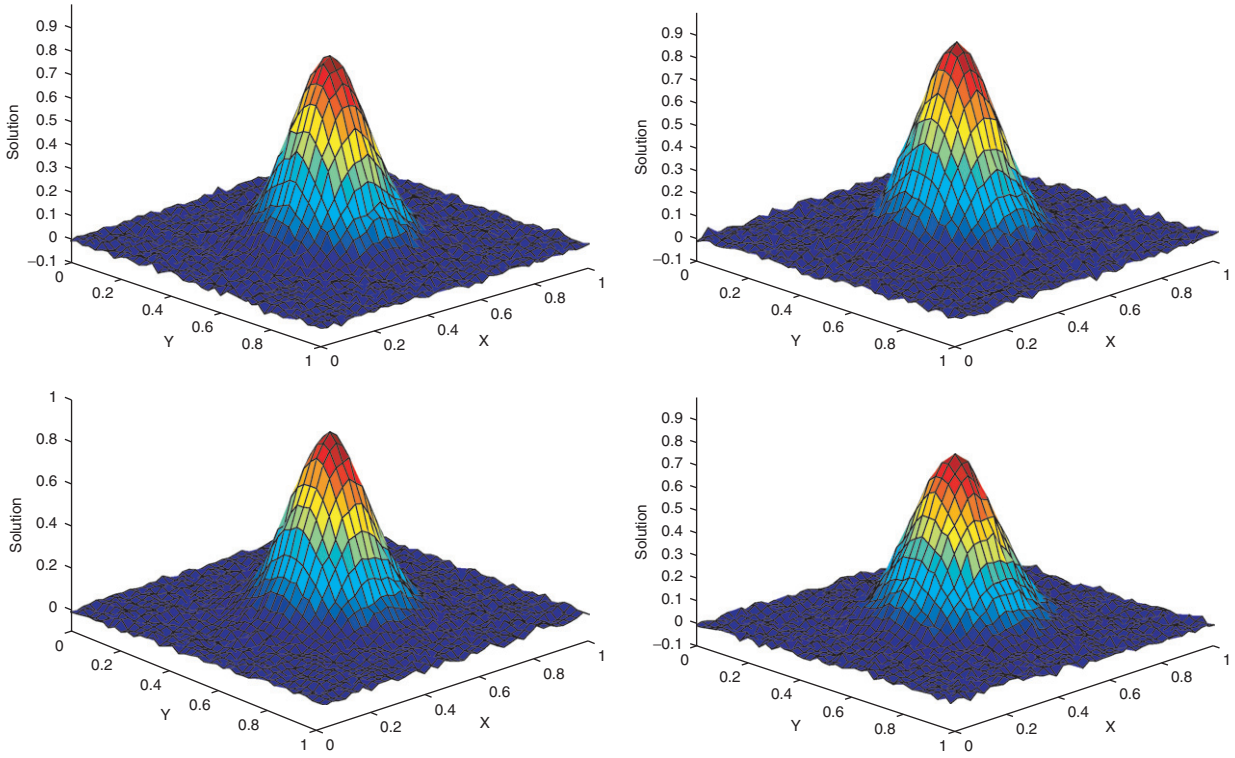

Fig. 7. Two-dimensional *Test* 1: four different simulations at time $t = 0.001$.

It is worth remarking that, the preprocessing *Step* 1 and the postprocessing *Step* 3 in our algorithm require very little computational work compared to the CPU time needed for solving the deterministic problems in *Step* 3. For instance, in all tests presented in this section, more than 67% of computational cost goes into solving *Step* 2. Therefore, reducing the CPU time in our algorithm can be hold by considering more efficient solvers for the deterministic reaction–diffusion equations. Recall that the chaos coefficients are computed in advance and stored in vectors to be used whenever a simulation of solution has to be repeated.

5.2. Two-dimensional results

We present numerical results for the two-dimensional formulation of *Test* 1, *Test* 2 and *Test* 3. The spatial domain is the unit square $\mathscr{D} = [0, 1] \times [0, 1]$ divided into uniform quadrilateral mesh with 40×40 gridpoints. For each test case we perform 50 different realizations and an averaged solution is calculated. To display the results we use the same tools as in the one-dimensional cases.

In Fig. 7 we report results at time $t = 0.001$ by executing four different realizations in *Test* 1. Fig. 8 shows the averaged solution (left column) and the evolution in time of a cross section at $y = 0.5$ (right column). The algorithm captures the long term behavior of the numerical averaged solution without breaking the symmetry in the computational domain or introducing oscillations in the averaged solutions.

The results for *Test* 2 are given in Figs. 9 and 10. Four selected simulations of the solution are shown in Fig. 9 at $t = 0.01$. As has been observed in the one-dimensional form of this test, the stochastic excitations produced by the reaction function are more detectable in the simulated solutions than in the previous test.

Finally, we present in Fig. 11 the simulated solutions for *Test* 3 by four different realizations at $t = 0.01$. As in *Test* 2, stochastic effects take place in the whole surface plots of the simulated solutions. In the left column of Fig. 12 we show the surface plot of the averaged solution at time $t = 0.001$, while in the right column we plot a cross-section at $y = 0.5$ for $t = 0$, 0.001 and 0.01. In this test case, the diffusion process of the initial Gaussian data is faster than those resulted from *Test* 2, see Figs. 10 and 12.

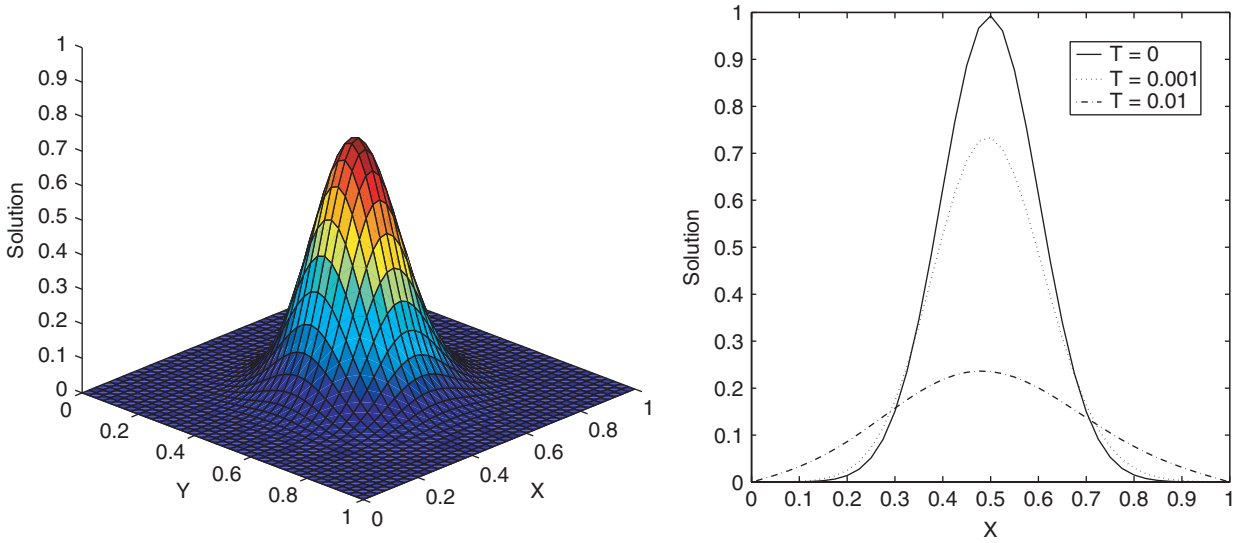

Fig. 8. Two-dimensional *Test* 1: surface plot of averaged solution at time $t = 0.001$ (left column) and its cross-section at $y = 0.5$ for different times (right column).

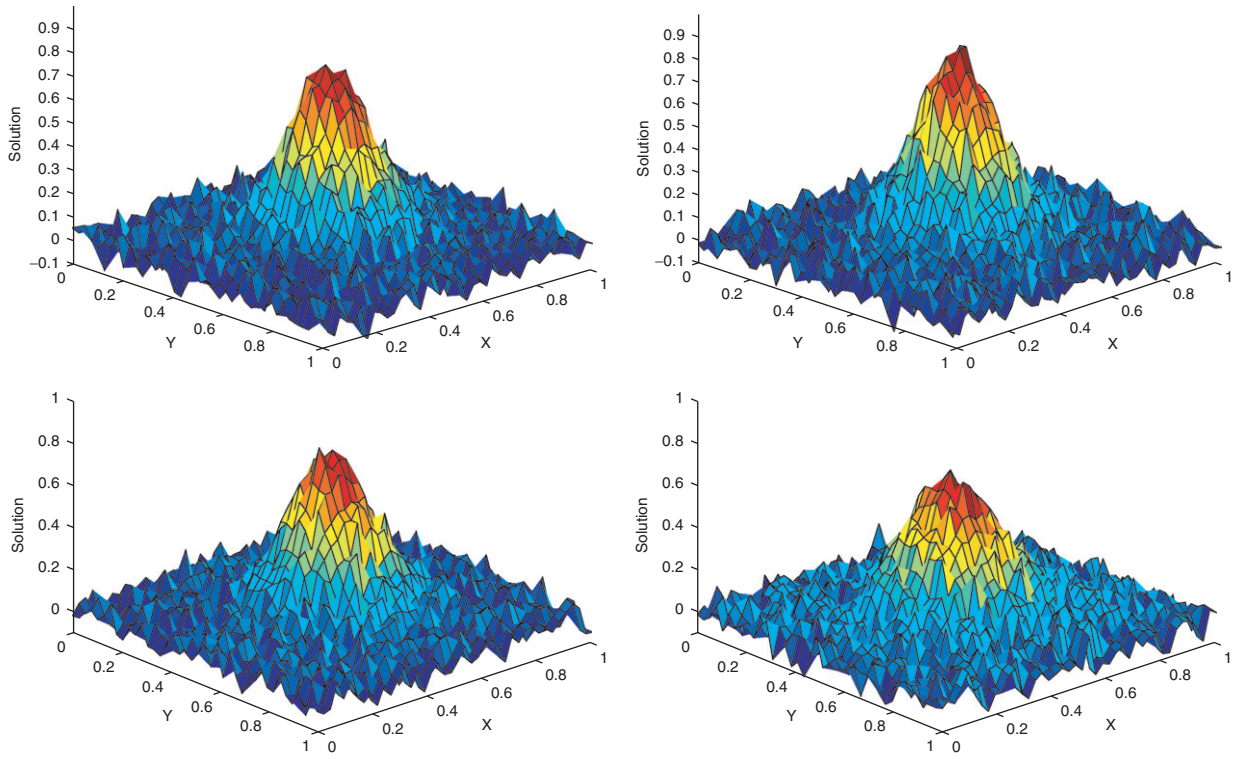

Fig. 9. Two-dimensional *Test* 2: four different simulations at time $t = 0.01$.

As a final remark, we would like to comment on the number of iterations needed in Bicgstab solver to converge. Since, the iterate mass matrix in *Test* 2 is symmetric and diagonal dominant, these properties make the convergence of Bicgstab solver faster with a mean of 4 iterations per time step. In *Test* 1 and *Test* 3, the iterate matrix in (13) loses the previous properties. For these test cases, the mean number of iterations in Bicgstab solver to reach the tolerance of

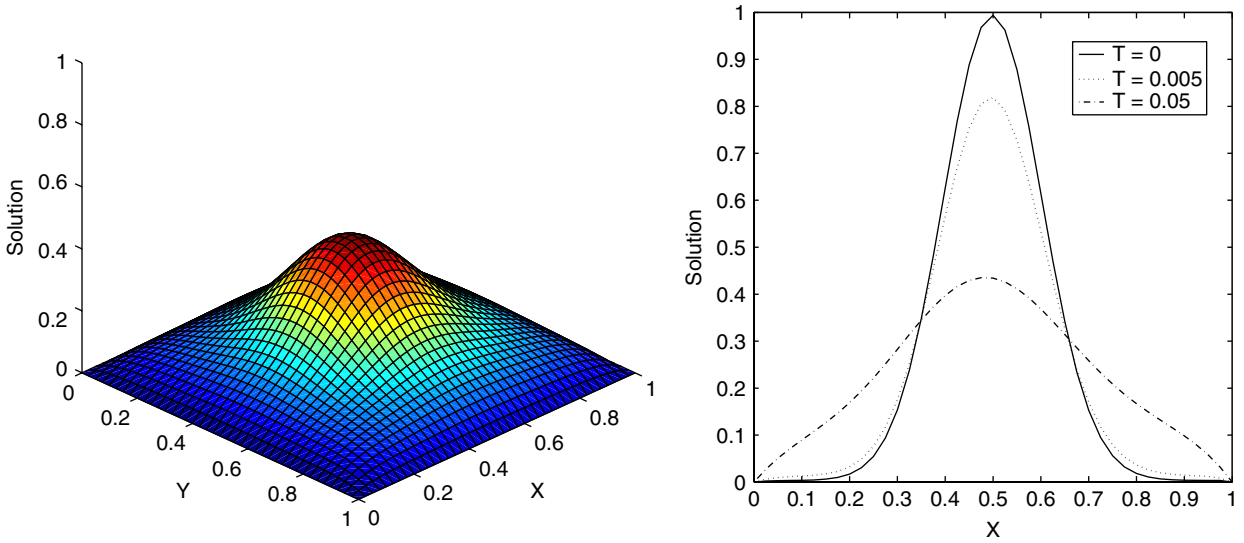

Fig. 10. Two-dimensional *Test* 2: surface plot of averaged solution at time $t = 0.05$ (left column) and its cross-section at $y = 0.5$ for different times (right column).

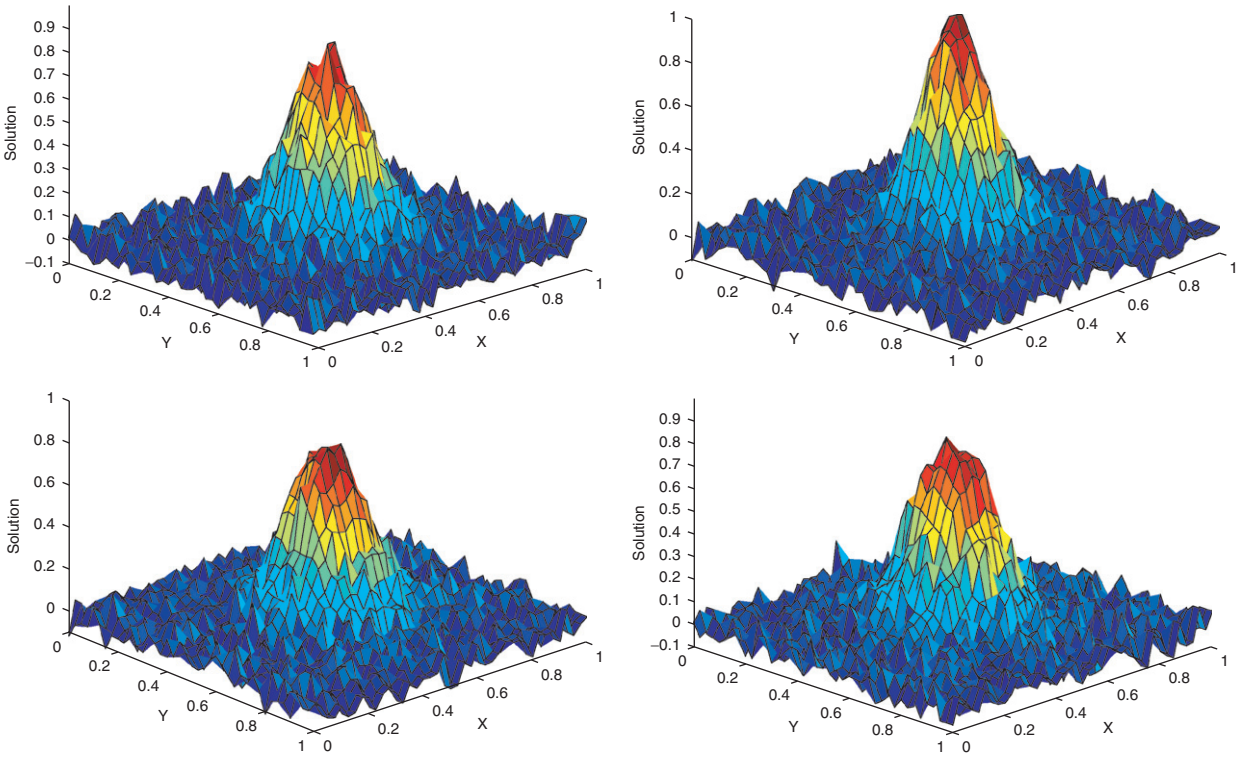

Fig. 11. Two-dimensional *Test* 3: four different simulations at time $t = 0.001$.

10^{-5} was 9 iterations per time step. Nevertheless, our algorithm can be executed with timestep sizes larger enough than for the explicit time integration methods. For instance, in *Test* 2 with 80 gridpoints, an explicit time stepping requires a timestep of order 10^{-9}. Therefore, for the same length of simulation, our algorithm uses fewer steps than an explicit method, thereby reducing the total computational cost tremendously.

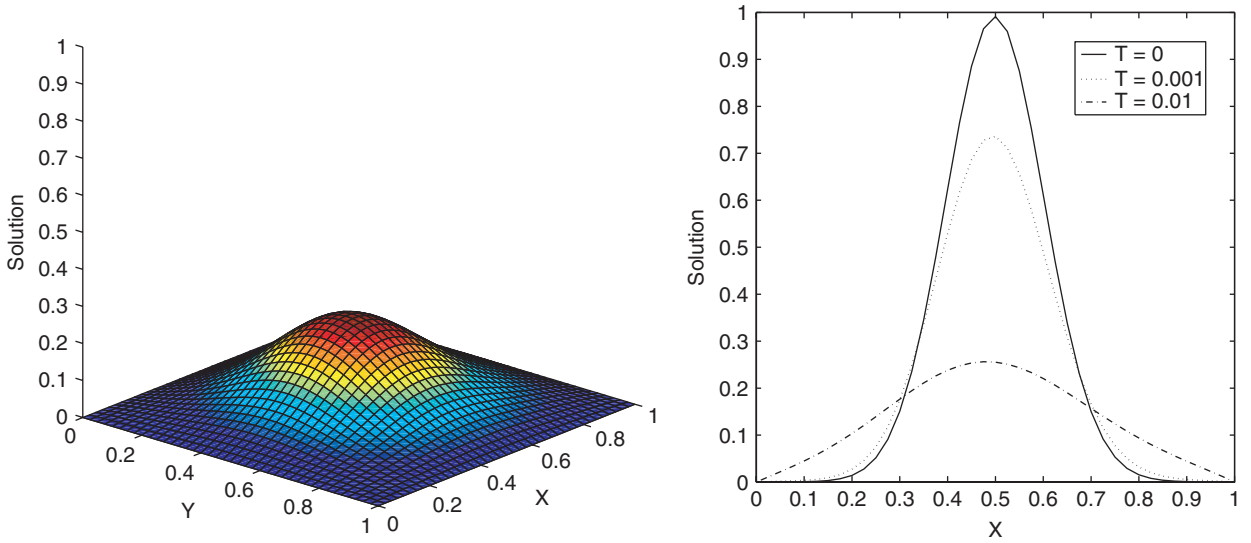

Fig. 12. Two-dimensional *Test* 3: surface plot of averaged solution at time $t = 0.01$ (left column) and its cross-section at $y = 0.5$ for different times (right column).

6. Concluding remarks

A robust numerical method for solving the one- and two-dimensional stochastic reaction–diffusion equations of Wick type has been developed and tested. The method combines the Wiener–Itô chaos expansion with a finite element method. An implicit time integration procedure is used to avoid the restriction on timesteps in computations.

The algorithm presented in this paper can be highly optimized for the vector computers, because this does not require nonlinear solvers and contains no recursive elements. The parallel implementation of the method requires only interprocessor communication to complete the matrix–vector and vector–vector products required at each iteration. Some difficulties arise from the fact that for efficient vectorization the data should be stored continuously within long vectors rather than two-dimensional arrays.

Although we have restricted our numerical computations to the linear scalar reaction–diffusion equations, the more important implication of our research concerns the use of Wick-stochastic finite element method for nonlinear coupled reaction–diffusion systems. Our future work is therefore to implement this method for solving nonlinear stochastic boundary value systems of Wick type in parallel computing using multilevel iterative solvers to speed up the time integration procedure.

References

[1] F. Benth, T. Theting, Some regularity results for the stochastic pressure equation of Wick-type, Stochastic Anal. Appl. 20 (2002) 1191–1223.
[2] F.E. Benth, J. Gjerde, Convergence rates for finite element approximations of stochastic partial differential equations, Stochastic Stochastic Rep. 63 (1998) 313–326.
[3] R. Dautray, J.L. Lions, Mathematical Analysis and Numerical Methods for Science and Technology, Springer, Berlin, 1993.
[4] Q. Du, T. Zhang, Numerical approximation of some linear stochastic partial differential equations driven by special additive noises, SIAM J. Numer. Anal. 40 (2002) 1421–1445.
[5] R. Ghanem, Ingredients for a general purpose stochastic finite elements implementation, Comput. Appl. Mech. Eng. 168 (1999) 19–34.
[6] H. Holden, Y. Hu, Finite difference approximation of the pressure equation for fluid flow in a stochastic medium: a probabilistic approach, Comm. Partial Differential Equations 21 (1996) 1375–1388.
[7] H. Holden, B. Øksendal, J. Ubøe, T. Zhang, Stochastic Partial Differential Equations: A Modeling, White Noise Functional Approach, Probability and its Applications, Birkhäuser, Basel, 1996.
[8] C.T. Kelly, Iterative Methods for Linear and Nonlinear Equations, SIAM, Philadelphia, 1995.
[9] Y. Kondratiev, P. Leukert, L. Striet, Wick calculus in Gaussian analysis, Acta Appl. Math. 44 (1996) 269–294.
[10] H. Manouzi, T. Theting, Mixed finite element approximation for the stochastic pressure equation of Wick type, IMA J. Numer. Anal. 24 (2004) 587–604.

[11] A. Stundzia, C. Lumsden, Stochastic simulation of coupled reaction–diffusion processes, J. Comput. Phys. 127 (1996) 196–207.
[12] D. Tartakovsky, A. Guadagnini, M. Riva, Stochastic averaging of nonlinear flows in heterogeneous porous media, J. Fluid Mech. 492 (2003) 47–62.
[13] T. Theting, Solving parabolic Wick-stochastic boundary value problems using a finite element method, Stochastic Stochastic Rep. 75 (2003) 57–92.
[14] H.A. Van der Vorst, BI-CGSTAB: a fast and smoothly converging variant of BI-CG for the solution of nonsymmetric linear systems, SIAM J. Sci. Statist. Comput. 13 (1992) 631–644.
[15] G. VAAge, Variational methods for PDEs applied to stochastic partial differential equations, Math. Scand. 82 (1998) 113–137.
[16] G. VAAge, Hilbert space methods applied to elliptic stochastic partial differential equations, Stochastic Anal. Related Topics 32 (1998) 281–294.